High P-T Raman study of transitions in relaxor multiferroic Pb(Fe0.5Nb0.5)O-3

Research article

Journal of RAMAN SPECTROSCOPY

Received: 30 March 2015 Revised: 29 June 2015 Accepted: 3 August 2015 Published online in Wiley Online Library: 2 September 2015

(wileyonlinelibrary.com) DOI 10.1002/jrs.4779

High *P–T* Raman study of transitions in relaxor multiferroic $Pb(Fe_{0.5}Nb_{0.5})O_3$

Brandon Wilfong,[a,b] Muhtar Ahart,[b]* Stephen A. Gramsch,[b] Chris Stock,[c] Xiaomin Li,[d] H. Luo[d] and Russell J. Hemley[b]

The vibrational and structural properties of $Pb(Fe_{0.5}Nb_{0.5})O_3$ have been investigated using Raman spectroscopy up to 40 GPa at 300 K and from 300 to 415 K at selected pressures. The measurements reveal three phase transitions, at 5.5, 8.7, and 24 GPa at room temperature. The temperature dependences of the spectra indicate transitions at 1.5 GPa, at 335 and 365 K. The results are consistent with the appearance of an intermediate tetragonal *P*4mm phase between the ferroelectric *R*3m and paraelectric *P*m-3m phases. A *P–T* phase diagram is proposed that allows further insight into the magnetoelectric coupling present in this material.

Additional supporting information may be found in the online version of this article at the publisher's web site.

Keywords: relaxor; multiferroic; high-pressure; two-phonon peak; phase transitions

Introduction

Multiferroic materials are interesting systems that exhibit transitions associated with both ferroelectric and magnetic order.[1] Generally, ferroelectric order is a product of relative structural shifts in the crystal lattice between negative and positive ions, which results in a dipole moment. Magnetism arises from electron ordering in ions with incomplete d orbitals. The combination of the two types of ordering within a material gives rise to interesting theoretical questions and can give rise to numerous applications for next generation electronics.[2] Lead ferroniobate, $Pb(Fe_{0.5}Nb_{0.5})O_3$ (PFN), falls into this class of multiferroic materials. PFN not only exhibits magnetic ordering but it also displays piezoelectric and pyroelectric properties, making it a promising material for use in multi-functional devices.[3,4] However, the combination of all of these properties introduces complexity that is not fully understood in this material.

Lead ferroniobate shows compositional chemical disorder on the B-site of its perovskite structure, so that if one of the unit cells of the structure has Fe^{3+} (d^5, S = 5/2) on its B-site, then any adjunct B-site may contain either magnetic Fe^{3+} or nonmagnetic Nb^{5+}. Such chemical disorder would yield a charge imbalance in the local structure. Consequently, in order to avoid such a charge imbalance, the system creates short-range ordered regions, which are embedded in the disordered matrix. These short-range ordered regions are associated with the polar properties and are referred to as polar nanoregions (PNR). Experimental evidence for the presence of locally ordered regions has been obtained from transmission electron microscopy, which indicates chemical short-range order in a prototype relaxor $Pb(Mg_{1/3}Nb_{2/3})O_3$ (PMN).[5] Specifically, 1 : 1 ordered domains 50 Å in size are formed in the material. These short-range ordered regions are the main cause of relaxor behavior in ferroelectric materials such as PFN.[6,7] Relaxor ferroelectrics are characterized by dispersion in the dielectric response that differs greatly from classic ferroelectrics. Relaxor ferroelectrics also have diffuse phase transitions and increased Raman activity due to relaxation of Raman selection rules.[8]

A previous x-ray diffraction study suggested a paraelectric *P*m-3m phase of PFN above $T_C = 376$ K, and a ferroelectric tetragonal phase in the temperature range 355–376 K with an assignment of *P*4mm.[9,10] A Neel temperature of 153 K for the antiferromagnetic to paramagnetic transition suggests a phase stable at ambient pressure between between 153 and 355 K, which has generated strong debate. Both rhomobohedral *R*3m and monoclinic *C*m space groups were assigned to this phase in previous studies.[9] The only previous high-pressure work on this material at room temperature suggests two phase transitions as a function of pressure: from ferroelectric *R*3m to ferroelectric *C*m at 5.0 GPa and from ferroelectric *C*m to ferroelectric *P*m at 8.5 GPa.[11] In the work of Kozlenko *et al.*,[11], the proposal that PFN does not lose ferroelectric properties at high pressure was based on speculation arising from earlier studies on lead titanate,[12,13] but is without any experimental evidence.

In order to further probe the properties of PFN, we used high-pressure and high-temperature techniques to drive physical and chemical changes within the material. This experimental approach provides insight into the *P-T* phase diagram of PFN so that multiferroic properties and signatures may be uncovered. Raman scattering was used in order to probe the local structure of the sample with changes in pressure and temperature.[14] Our experimental setup has allowed us to measure the lowest wavenumber peaks

* *Correspondence to: Muhtar Ahart, Geophysical Laboratory, Carnegie Institution of Washington, 5251 Broad Branch Rd. NW, Washington, DC 20015, USA. E-mail: maihaiti@carnegiescience.edu*

a *Washington College, 300 Washington Ave., Chestertown, MD 21620, USA*

b *Geophysical Laboratory, Carnegie Institution of Washington, 5251 Broad Branch Rd. NW, Washington, DC 20015, USA*

c *School of Physics and Astronomy, University of Edinburgh, Edinburgh EH9 3JZ, UK*

d *Shanghai Institute of Ceramics, Chinese Academy of Sciences, Shanghai 201800, China*

down to ~20 cm^{-1}, which were not measured in earlier work.[11] These low wavenumber peaks play an important role in determining phase transitions of classic ferroelectrics via a soft optical mode.[15] In relaxor systems, the soft modes are over-damped because of the coupling between soft-modes and PNRs.[16] However, these modes still may play an important role in discerning phase transitions. It is important to note that due to the relaxor ferroelectric behavior of PFN and the formation of polar nanoregions because of B-site perovskite disorder, the local structure will differ from the average structure. In addition, as shown in previous studies,[17] important information can be extracted from the Raman intensity for perovskite-like materials. Raman scattering is therefore an invaluable tool for extracting information from these complex systems.

Experimental techniques

The PFN sample was synthesized using a procedure similar to that described in detail in a previous study.[11] The single crystal sample, with a lateral size of 40 μm and thickness of 15 μm, was loaded into a diamond anvil cell (DAC). A 25-μm-thick stainless steel gasket with a 13-μm-diameter hole was used as the sample chamber. Raman grade diamond anvils with a culet size of 300 μm were used with a symmetric DAC. Two different types of pressure medium were used. A 4:1 methanol/ethanol mixture was used for 0–12 GPa experiments and argon for the 7–40 GPa data set as well as for all temperature-dependent measurements.[18] Pressure was determined in both cases by the ruby fluorescence technique.[19,20] As examples, the photo-images of loaded samples are shown in Fig. S1(Supporting Information).[21]

Temperature was controlled by the use of a Variac-powered bulk DAC heating apparatus that was reliable in heating the entire sample in our desired temperature range from ambient temperature to about 415 K. A K-type (Chromel-Alumel) thermocouple was used to determine the temperature. Four distinct pressures were chosen: 2.0, 2.9, 4.0, and 7.5 GPa. At these selected pressures, the cell was heated using the bulk heater, and the Raman spectra were measured at approximately 10 K increments. Pressure changes in the system during heating were measured via the ruby fluorescence temperature-dependent technique.[20]

All Raman spectra were measured using a Princeton Instruments Acton SP2300 spectrometer paired with a CCD and a solid-state diode excitation laser with 532 nm source wavelength. Laser power is about 7 mW before entering the DAC. For all experiments, an 1800BLZ grating was used, and the Raman signal was measured in the backscattering geometry with an average collection time of 300 s. The use of ultra-fine notch filters (Ondax Inc.) allowed measurements of spectra to approximately 20 cm^{-1}. We used a long working distance, Mitutoyo 20X objective with a numerical aperture of 0.28, and our microscopic Raman system has a spatial resolution of 1.14 μm.

Results and discussion

Pressure dependence

The Raman spectra of PFN were first measured at selected pressures at room temperature. A raw spectral pressure evolution is shown in Fig. S2 (Supporting Information)[21], and corrected spectral evolution is shown in Fig. 1. Some of the details of the spectra

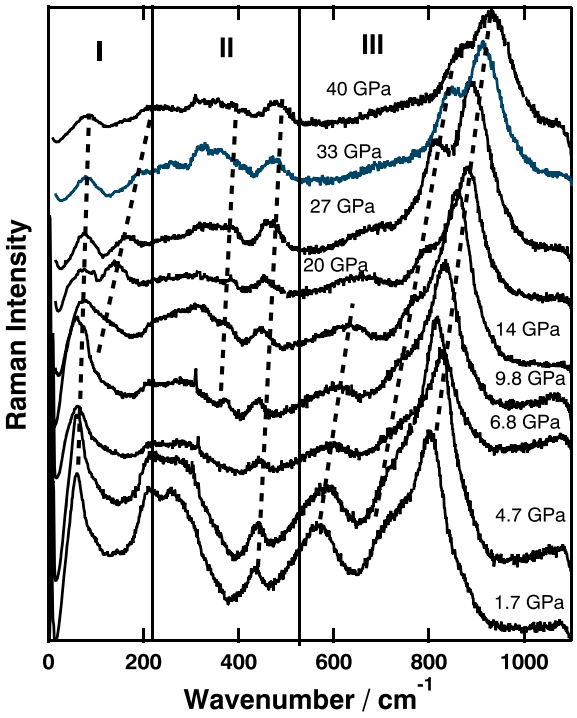

Figure 1. Typical Raman spectra of $Pb(Fe_{0.5}Nb_{0.5})O_3$ at selected pressures and room temperature. The spectra were corrected by the thermal Bose–Einstein population factor. The spectra can be separated into three regions: below 200 cm^{-1} and indicated as I in the figure; between 200 and 450 cm^{-1} and indicated as II; and the region above 450 cm^{-1} indicated as III. It is clear that the lowest wavenumber peak shows drastic broadening above 5 GPa and a splitting above 8 GPa, indicative of the structural transitions. Dashed lines are used to emphasize peak position trends between spectrum.

corrections and Raman active modes in relevant space groups (Table S1) are given in the Supporting Information.[21]

There are three distinct regions denoted I, II, and III for ease of analysis (Fig. 1). Region I denotes low wavenumber peaks, attributed to localization of Pb atoms,[22] from 20 to 200 cm^{-1}; these showed a drastic change as a function of pressure as emphasized in Fig. S3 (Supporting Information). The lowest peak at 60 cm^{-1} decreased in intensity throughout, and the formation of a new peak occurred approximately 105 cm^{-1} at 8.5 GPa; hardened with pressure and increased in intensity until 24 GPa before weakening. Region II includes the middle wavenumber peaks. These are due to Pb–O bond stretching modes from 200 to 400 cm^{-1} and Fe–O/Nb–O bending modes[23] from 400 to 530 cm^{-1}. In this region, there are three prominent features: the broad band from 200 to 325 cm^{-1}, which decreased in intensity as pressure increased, the formation of a new peak at around 6 GPa and centered at 378 cm^{-1} that displayed marginal pressure evolution, and the peak at 435 cm^{-1}, which hardened slightly and showed some broadening with pressure. Region III shows the highest wavenumber modes, which also showed some significant changes with pressure. All of these modes are attributed to BO_6 (B = Fe or Nb) octahedral vibrations.[23] Notably, the broad band from 530 to 630 cm^{-1} showed a decrease in intensity as well as hardening with pressure, while the peak centered at 800 cm^{-1} showed virtually no change in intensity or width with pressure but did display considerable hardening.[23] The most distinct change is the formation of a shoulder on the 800 cm^{-1} peak at about 8.5 GPa, which increased in intensity through its pressure evolution and displayed hardening behavior similar to the peak centered at 800 cm^{-1}.

The correct method for analyzing the Raman spectra of relaxor ferroelectrics is still open to debate because of their inherent compositional complexity as well as chemical and structural disorder in the lattice. These types of disorder relax the Raman selection rules and cause broadening of spectral peaks. The observed Raman spectra from relaxor ferroelectrics do not clearly represent the phonon density of states or regular vibrational spectra exclusively. However, many previous studies have analyzed the Raman spectra of relaxor ferroelectrics by the use of the damped harmonic oscillator model.[24,25] In addition, the low temperature Raman spectra of PMN[23] or PFN[26] showed sharper peaks than that of room temperature spectra, indicating that the observed spectra represented the vibrational spectra predominantly at low temperature. However, because of the broad nature of the Raman spectra of these materials, it will be difficult to use the damped harmonic oscillation model to analyze the observed Raman spectra.

In order to understand the structural transitions, we carefully inspected the spectrum at each pressure and temperature to obtain the spectral evolution as the function of pressure and temperature. The detailed procedures are provided in the Supporting Information.[21] An example of fitting is shown in Fig. S4 (Supporting Information). It should be noted that because the Raman selection rules are relaxed in these chemically disordered relaxor perovskite systems, more peaks are active than are theoretically allowed based on the space group assignments. In Fig. S3 (Supporting Information), the low wavenumber region of the spectra are shown at the selected pressures and at room temperature. It is clear that the lowest wavenumber peak shows drastic broadening above 5.5 GPa indicative of a transition; subsequently, same band shows splitting above 8 GPa indicative of another transition. In Fig. 2, a peak positions of low wavenumber modes are shown as a function of pressure at room temperature.

All modes displayed hardening behavior; and the behavior of some particular peaks indicated phase transitions. It should be noted that because of the relaxor behavior of PFN, phase transitions are diffuse, unlike classic ferroelectrics, which made detecting phase transitions more difficult and less straightforward. Nonetheless, particular peak behaviors were evaluated as a function of pressure evolution to detect discontinuities.

Analysis of the corrected spectra qualitatively showed possible phase transitions at 5.5, 8.5, and 24 GPa and these are supported by the analysis of peak position as a function of pressure. From 5.5 to 8.7 GPa (Fig. 2), all three low wavenumber mode showed a drastic change in slope and rapid softening, while above 8.7 GPa, all three modes began to harden and showed an increase in slope. The discontinuity at 24 GPa is emphasized in Fig. 2. All middle wavenumber peaks showed rapid hardening from 8.7 to 24 GPa, but at pressures higher than 24 GPa, they showed a drastic change in slope. These sets of peaks are also of special interest for perovskite ferroelectrics.[5] The 8.7 GPa phase transition is also characterized by the appearance of a new peak at 375 cm^{-1}; while the 5.5 GPa transition is characterized by the weakening of the highest wavenumber peak at 900 cm^{-1}. Overall, these results suggest three phase transitions at room temperature as a function of pressure, at 5.5, 8.7, and 24 GPa.

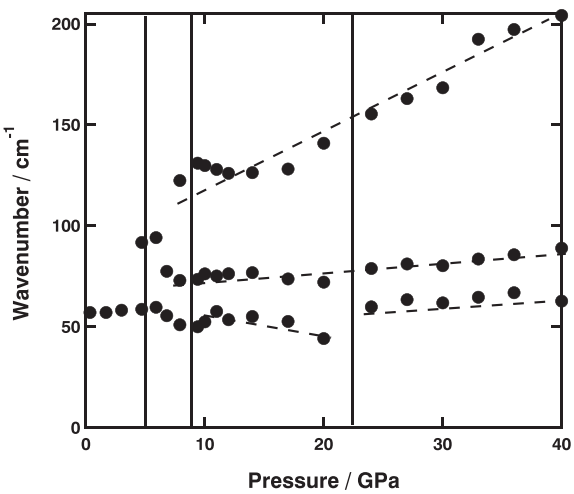

Figure 2. Peak positions of low wavenumber modes as the function of pressure at room temperature.

Temperature dependence

Four distinct pressures (2.0, 2.9, 4.0, and 7.5 GPa) were selected to measure the temperature dependence of the Raman signal from ambient temperature to 415 K. Similar experimental procedures were followed for the pressure dependence experiment, but it is important to note that a steady temperature was approximated between measurements using the selective output control of the Variac-powered bulk heating apparatus. Qualitative analysis of spectra as a function of temperature is less fruitful than that of pressure and should be attributed to the more dynamic effect of pressure on crystal systems. One temperature evolution in particular, the 2.0 GPa base pressure set, showed a distinct spectral change. We attribute this to the continuation of the tetragonal *P*4mm phase proposed by Bonny *et al.*[9] at ambient pressure. This spectral evolution is shown in Fig. 3.

The remaining temperature evolution at the selected pressures shows minimal spectral change. The peaks that showed the clearest discontinuities for each pressure as a function of temperature are shown in Fig. 4 and labeled accordingly. First, we evaluate the temperature dependence of the Raman spectra for the pressure of 2.0 GPa. Figure 3 shows two phase transitions within the temperature evolution as inferred from the behavior of middle wavenumber peaks with temperature. Two phase transitions at this pressure and temperature evolution support the conclusion of Bonny *et al.*[9] for an intermediate tetragonal phase from 355 to 376 K. Our data support the persistence of this intermediate tetragonal phase, even at this increased pressure, between 335 and 365 K.

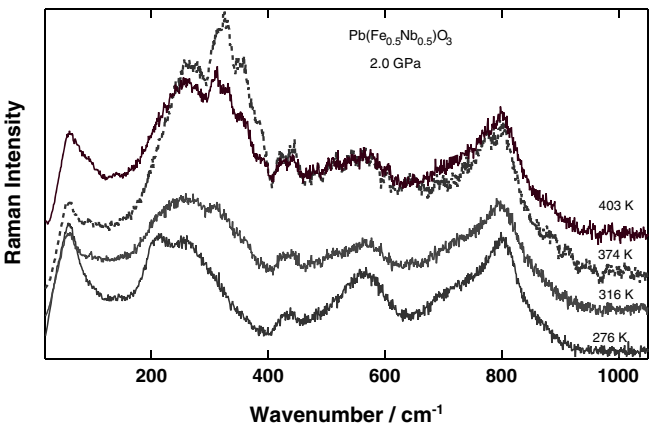

Figure 3. Raman spectra of $Pb(Fe_{0.5}Nb_{0.5})O_3$ at selected temperatures at 2.0 (±0.5) GPa. Spectra were corrected by the thermal Bose–Einsten population factor. The spectral range was from 20 to 1100 cm^{-1} via our experimental setup. A clear qualitative change is seen in the range of 369–374 K.

Higher than 365 K, the system adapts a cubic structure in agreement with previous work.[9] At the next base pressure, 2.9 GPa, we observe only one phase transition at 348 K, best represented by the temperature dependence of the lowest wavenumber peaks. Only one phase transition at this pressure suggested the extinction of the tetragonal phase. At 4.0 GPa, the temperature dependence displayed one phase transition and followed the trend observed at 2.9 GPa. One phase transition justified the previous assumption concerning the extinction of the tetragonal phase, and the transition to the cubic phase showed an appreciable decrease in temperature as pressure was increased. The next base pressure chosen was 7.5 GPa, and this pressure gap was selected purposefully in order to probe the region between 5.5 and 8.7 GPa at ambient temperature for possible phase transitions. Similar to previous measurements, only one phase transition was noted at 332 K, to the cubic phase.

Impact of magnetic Fe^{3+}

Unlike other well-known lead oxide perovskites, PFN contains a magnetic B-site ion (Fe^{3+}, d^5, S = 5/2). It is this magnetic moment that plays an important role in the possible magnetoelectric coupling within the system. As proposed in the work of Garcia *et al.*,[26] the spin–phonon coupling[27] could be the origin for the anomalous softening behavior of the Raman bands below the Neel temperature (T_N = 153 K) at ambient pressure. Such spin–phonon coupling could originate from the Fe–O–Nb stretching modes, which in turn would modulate the Fe–O–Nb–O–Fe superexchange interactions in the antiferromagnetic-ordered phase below T_N. In addition, in a previous study,[28] the authors report dielectric anomalies around the Neel temperature indicative of strong magnetoelectric coupling in PFN below T_N.

Because our measurements were limited to room temperature and above, we were not able to obtain direct information regarding the magnetic and ferroelectric coupling. However, by directly comparing the pressure evolution of Raman spectra for PFN and $Pb(Sc_{0.5}Nb_{0.5})O_3$ (PSN), where PSN contains Sc^{3+}, which has a d^0 configuration and therefore no magnetic moment,[15] we can obtain useful insight into the effect of the Fe^{3+} ion. A comparison of spectra at ambient pressure is shown in Fig. 5. Although both PFN and PSN are ferroelectric (*R*3m) at 300 K and ambient pressure, the Raman spectrum of PFN shows much broader features than that of PSN. In the work of Blinc *et al.*,[29] the authors proposed that PFN shows antiferromagnetic ordering below T_N and short-range magnetic ordering above T_N, which originates from the formation of superparamagnetic clusters. These superparamagnetic clusters may further interfere with the Raman selection rule, in addition to the effect of PNR, and cause further broadening of Raman bands as seen in Fig. 5.

The peak appearing around 1100 cm^{-1} was assigned to a two-phonon process due to the interaction of Fe-sublattices.[26] The

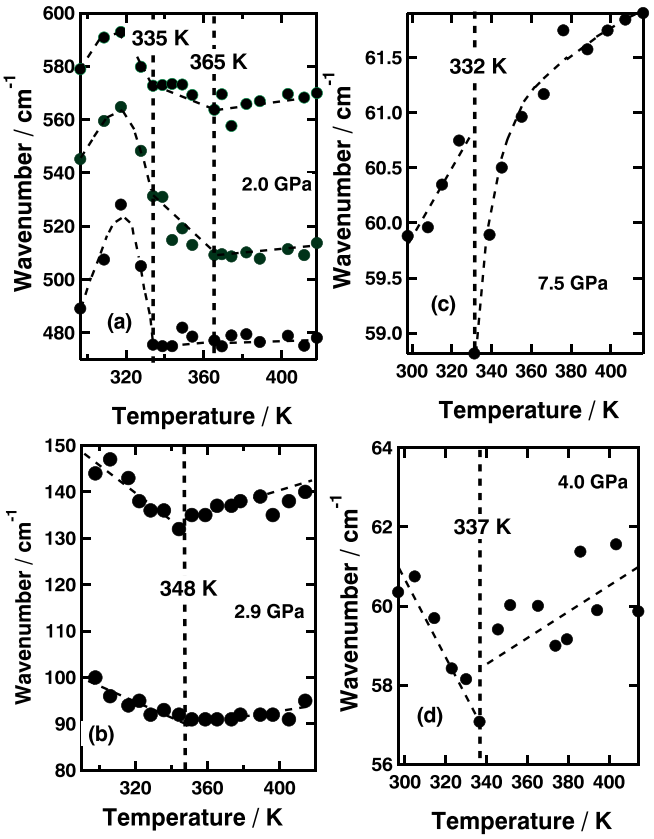

Figure 4. Temperature evolution of peak position for all four base pressures: (a) 2.0 (±0.5) GPa, (b) 2.9 (±0.4) GPa, (c) 7.5 (±0.1) GPa, and (d) 4.0 (±0.2) GPa. Vertical dashed lines denote possible phase transitions marked by peak position discontinuities as a function of temperature; the temperature at these proposed phase transitions are marked as well. Other dashed lines are used to emphasize peak position trends between measurements.

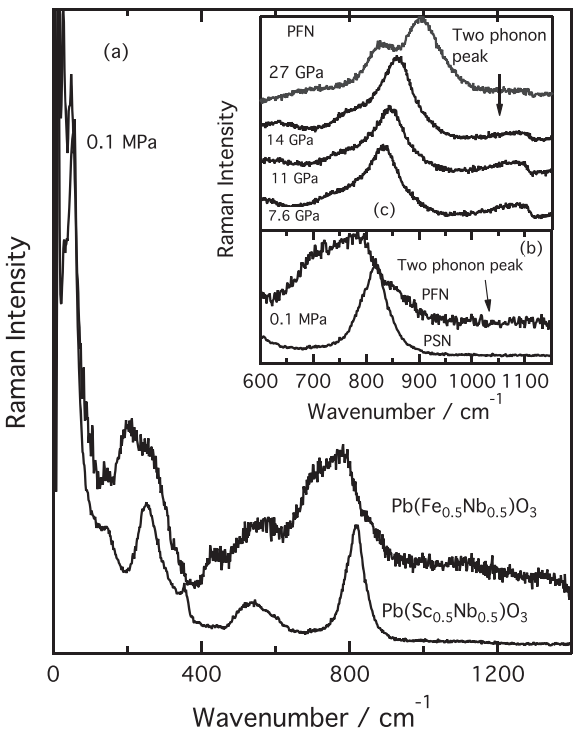

Figure 5. A comparison of Raman spectra for $Pb(Fe_{0.5}Nb_{0.5})O_3$ (PFN) and $Pb(Sc_{0.5}Nb_{0.5})O_3$ (PSN). PFN contains Fe^{3+}, which has a d^5 configuration and Fe^{3+} sublattices, which form the superparamagnetic clusters in addition to the PNRs; this causes broadening of the Raman bands. PSN however contains Sc^{3+}, which has a d^0 configuration and therefore no magnetic moment. Both systems have the same B-site disorder as well as secondary B-site cation, Nb^{5+}. A comparison of the two Raman spectra may help to elucidate the impact of magnetic Fe^{3+} on the system and possible magnetoelectric coupling. (b) Comparison of two-phonon region between PFN and PSN at ambient pressure. (c) Two-phonon interaction mode due to Fe-sublattice interactions at 1100 cm^{-1} at selected pressures. The two-phonon mode is clearly evident up to 14 GPa and its intensity becomes weaker with increased pressure above 14 GPa.

intense two-phonon peak at 10 K decreases with increasing temperature but persists up to room temperature. We observed this two-phonon peak up to 14 GPa at room temperature, but above 14 GPa, the two-phonon peak appeared weaker as shown in Fig. 5 (b) and (c). This two-phonon peak was also found in studies of multiferroic $BiFeO_3$[30] and was modeled with respect to the FeO_6 octahedral rotations, which in turn affect the superexchange because superexchange is heavily dependent on bond angles. The same consideration would follow for PFN as mentioned previously, so that this octahedral rotation plays a critical role in the weak magnetism of PFN above the Neel temperature.[30] Due to the increasing evidence for the importance of this two-phonon peak in terms of the superexchange in antiferromagnetism as well as the elucidation of magnetoelectric coupling, we suggest the further investigation of this particular peak.

When comparing the pressure evolution of Raman spectra in both PFN and PSN systems, the qualitative differences are in the lowest wavenumber peaks (centered at 50 cm^{-1}), which correspond to localized Pb atomic movements, and the highest wavenumber peaks, which correspond to BO_6 breathing modes. In PFN, we see the splitting of the lowest wavenumber mode starting at around 9 GPa, whereas in PSN[25] there is no change in the lowest wavenumber mode apart from a slight intensity change. Both PFN and PSN[25] show the formation and hardening of the shoulder peak at 780 cm^{-1}, but in the PFN system, we see a much higher intensity shift with pressure evolution.

P–T phase diagram

We have combined in Fig. 6 our pressure and temperature experiments into a *P–T* phase diagram that depicts all phase transitions from our experimental data as well as those from previous work. We have supported previous work for the appearance of three phase transitions from room temperature to 415 K in the low pressure region below 3 GPa. Our data on the temperature evolution at 2.0 GPa ± 0.5 GPa showed the appearance of the intermediate tetragonal *P*4mm phase observed also by Bonny *et al.*[9] The correct space group assignment for the ferroelectric *R*3m phase is still debated. Kozlenko *et al.*[11] proposed space group assignments, based on both X-ray and Raman data for the 6–8 GPa regions at room temperature as well as the region above 8.7 GPa at room temperature, as *C*m and *P*m, respectively. There clearly is a need for additional second harmonic generation experiments, so that these regions may be conclusively assigned as ferroelectric. The assignments by Kozlenko *et al.*[11] contradict the conventional understanding that ferroelectricity is suppressed at high pressure. The phase diagram illustrates that the ferroelectric phase at room temperature and pressure covers a wide region from 175 to 330 K and 0–5 GPa. This region is one of the most prominent for magnetoelectric coupling because of the transitions from antiferromagnetic to ferroelectric behavior. For application to technical devices, PFN offers a wide range of temperature and pressure at which this coupling is possible.

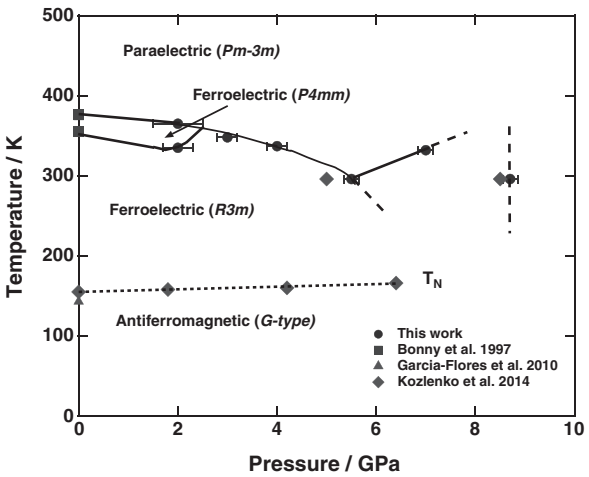

Figure 6. *P–T* phase diagram of $Pb(Fe_{0.5}Nb_{0.5})O_3$. Pressure error bars for temperature evolution as well as experimental error are displayed by horizontal bars. Temperature error bars are contained within the symbol size. All solid lines show expected phase boundaries while dotted lines are extrapolated phase boundaries via data trends. The phase boundary at 8.7 GPa is placed only to acknowledge its existence and its shape is arbitrary. Space group assignments are tentative as the nature of the ferroelectric *R*3m phase is still debated.

Conclusions

We employed Raman scattering combined with DAC methods to study the vibrational and structural properties of PFN from ambient to 40 GPa and 300 K to 415 K at selected pressures. We found that structural transitions occurred at 5.5, 8.7, and 24 GPa at room temperature. The two-phonon peak at 1100 cm^{-1}, originating from the Fe sublattice, may correlate to the superparamagnetic clusters and show weak pressure dependence up to 14 GPa at room temperature. Because of the existence of superparamagnetic clusters in addition to the PNRs, the observed Raman spectra show much broader features than that of classical nonmagnetic relaxors, such as PSN. Two phase transitions are noted at 1.5 GPa, at 335 and 365 K, consistent with the appearance of an intermediate tetragonal phase between ferroelectric to paraelectric phases. At 2.9, 4.0, and 7.5 GPa, the material shows only one phase transition which occurs at 337, 348, and 332 K respectively. A *P–T* phase diagram is provided that highlight the region magnetoelectric coupling at ambient conditions.

Acknowledgements

This work was supported by the US Department of Energy through the Carnegie/DOE Alliance Center (DE-NA0002006), and the Balzan. This work is also partially supported by the Ministry of Science and Technology of China through 973 program (Nos. 2013CB632902-3, 2013CB6329052, and 2013CB632906).

References

[1] S.-W. Cheong, M. Mostovoy, *Nature Mater.* **2007**, *21*, 13.
[2] D. Khomskii, *Phys.* **2009**, *2*, 20.
[3] V. Isupov, *Ferroelectrics.* **2003**, *289*, 131.
[4] G. A. Smolenski , I. E. Chupis, *Sov. Phys. Usp.* **1982**, *25*, 475.
[5] H. B. Krause, J. M. Cowley, J. Wheatley, *Acta Cryst.* **1979**, *A35*, 1015.
[6] B. P. Burton, E. Cockayne, U. V. Waghmare, *Phys. Rev. B.* **2005**, *72*, 064113.
[7] S. Tinte, B. P. Burton, E. Cockayne, U. V. Waghmare, *Phys. Rev. Lett.* **2006**, *97*, 137601.
[8] S. Kojima, R. Ohta, T. Ariizumi, J. Zushi, *J. Phys. Conference Series.* **2013**, *428*, 012027.
[9] V. Bonny, M. Bonin, P. Sciau, K. J. Schenk, G. Chapuis, *Solid state commun.* **1997**, *102*, 347.
[10] N. Lampis, P. Sciau, A. G. Lehmann, *J. Phys.: Condensed Matter.* **1999**, *11*, 3489.
[11] D. P. Kozlenko, S. E. Kichanov, E. V. Lukin, N. T. Dang, L. S. Dubrovinsky, H.-P. Liermann, W. Morgenroth, A. A. Kamynin, S. A. Gridnev, B. N. Savenko, *Phys. Rev. B.* **2014**, *89*, 174107.

[12] I. A. Kornev, L. Bellaiche, P. Bouvier, P.-E. Janolin, B. Dkhil, J. Kreisel, *Phys. Rev. Lett.* **2005**, *95*, 196804.
[13] P.-E. Janolin, P. Bouvier, J. Kreisel, P. A. Thomas, I. A. Kornev, L. Bellaiche, W. Crichton, M. Hanand, B. Dkhil, *Phys. Rev. Lett.* **2008**, *101*, 237601.
[14] R. Loudon, *Adv. Physiol. Educ.* **1964**, *13*, 423.
[15] J. F. Scott, *Rev. Mod. Phys.* **1974**, *46*, 83.
[16] P. M. Gehring, S. Wakimoto, Z.-G. Ye, G. Shirane, *Phys. Rev. Lett.* **2001**, *87*, 277601.
[17] A. Slodczyk, M.-H. Limage, P. Colomban, O. Zaafrani, F. Grasset, J. Loricourt, B. Sala, *J. Raman Spectrosc.* **2011**, 42.
[18] A. Jayaraman, *Rev. Mod. Phys.* **1983**, *55*, 65.
[19] H. Mao, J.-A. Xu, P. Bell, *J. Geophys. Res.: Solid Earth.* **1986**, *91*(B5), 4673.
[20] S. Rekhi, L. S. Dubrovinsky, S. K. Saxena, *High Temperatures-High Pressures.* **1999**, *31*, 299.
[21] Supplemental Materials. It includes photo-image of loaded samples; spectra analyses (fitting procedure); and normal modes in the relevant space groups.
[22] M. Correa, A. Kumar, S. Priya, R. S. Katiyar, J. F. Scott, *Phys. Rev. B.* **2011**, *83*, 014302.
[23] S. A. Prosandeev, E. Cockayne, B. P. Burton, S. Kamba, J. Petzelt, Y. Yuzyuk, R. S. Katiyar, S. B. Vakhrushev, *Phys. Rev. B.* **2004**, *70*, 134110.
[24] R. Haumont, P. Gemeiner, B. Dkhil, J. M. Kiat, A. Bulou, *Phys. Rev. B.* **2006**, *73*, 104106.
[25] B. J. Maier, N. Waeselmann, B. Mihailova, R. J. Angel, C. Ederer, C. Paulmann, M. Gospodinov, A. Friedrich, U. Bismayer, *Phys. Rev. B.* **2011**, 84,174104.
[26] A. F. Garcia, D. A. Tenne, Y. J. Choi, W. J. Ren, X. X. Xi, S. W. Cheong, *J. Phys. Condens. Matter* **2011**, *23*, 015401.
[27] C. Stock, S. R. Dunsiger, R. A. Mole, X. Li, H. Luo, *Phys. Rev. B.* **2013**, *88*, 094105.
[28] Y. Yang, J. -M. Liu, H. B. Huang, W. Q. Zou, P. Bao, Z. G. Liu, *Phys. Rev. B.* **2004**, *70*, 132101.
[29] R. Blinc, V. L. Laguta, B. Zalar, B. Zupancic, M. Itoh, *J. Appl. Phys.* **2008**, *104*, 084105.
[30] M. O. Ramirez, M. Krishnamurthi, S. Denev, A. Kumar, S. Y. Yang, Y. H. Chu, E. Saiz, J. Seide, A. P. Pyatakov, A. Bush, D. Viehland, J. Orenstein, R. Ramesh, V. Gopalan, *Appl. Phys. Lett.* **2008**, *92*, 022511.

Supporting information

Additional supporting information may be found in the online version of this article at the publisher's web site.